

Published in final edited form as:

J Control Release. 2019 June 22; 307: 331–341. doi:10.1016/j.jconrel.2019.06.025.

Tailoring the lipid composition of nanoparticles modulates their cellular uptake and affects the viability of triple negative breast cancer cells

Hanan Abumanhal-Masarweh^{1,2}, Dana da Silva¹, Maria Poley¹, Assaf Zinger¹, Evgenya Goldman¹, Nitzan Krinsky¹, Ron Kleiner¹, Gal Shenbach¹, Josh E. Schroeder³, Jeny Shklover¹, Janna Shainsky-Roitman¹, Avi Schroeder^{1,*}

¹Laboratory for Targeted Drug Delivery and Personalized Medicine Technologies, Department of Chemical Engineering, Technion—Israel Institute of Technology, Haifa 32000, Israel

²Russell Berrie Nanotechnology Institute, The Norman Seiden Multidisciplinary Graduate program, Technion—Israel Institute of Technology, Haifa 3200, Israel

³Department of Orthopedic Surgery, Hadassah Medical Center, Jerusalem 91120, Israel

Abstract

Lipid nanoparticles are used widely as anticancer drug and gene delivery systems. Internalizing into the target cell is a prerequisite for the proper activity of many nanoparticulate drugs. We show here, that the lipid composition of a nanoparticle affects its ability to internalize into triple-negative breast cancer cells. The lipid headgroup had the greatest effect on enhancing cellular uptake compared to other segments of the molecule. Having a receptor-targeted headgroup induced the greatest increase in cellular uptake, followed by cationic amine headgroups, both being superior to neutral (zwitterion) phosphatidylcholine or to negatively-charged headgroups. The lipid tails also affected the magnitude of cellular uptake. Longer acyl chains facilitated greater liposomal cellular uptake compared to shorter tails, 18:0>16:0>14:0. When having the same lipid tail length, unsaturated lipids were superior to saturated ones, 18:1>18:0. Interestingly, liposomes composed of phospholipids having 14:0 or 12:0-carbon-long-tails, such as DMPC and DLPC, decreased cell viability in a concentration dependent manner, due to a destabilizing effect these lipids had on the cancer cell membrane. Contrarily, liposomes composed of phospholipids having longer carbon tails (16:0 and 18:0), such as DPPC and HSPC, enhanced cancer cell proliferation. This effect is attributed to the integration of the exogenous liposomal lipids into the cancer-cell membrane, supporting the proliferation process. Cholesterol is a common lipid additive in nanoscale formulations, rigidifying the membrane and stabilizing its structure. Liposomes composed of DMPC (14:0) showed increased cellular uptake when enriched with cholesterol, both by endocytosis and by fusion. Contrarily, the effect of cholesterol on HSPC (18:0) liposomal uptake was minimal. Furthermore, the concentration of nanoparticles in solution affected their cellular uptake. The higher the concentration of nanoparticles the greater the *absolute* number of nanoparticles taken up per cell. However, the *efficiency* of nanoparticle uptake, i.e. the percent of nanoparticles taken up by cells, decreased as the concentration of nanoparticles increased. This

* avids@technion.ac.il.

study demonstrates that tuning the lipid composition and concentration of nanoscale drug delivery systems can be leveraged to modulate their cellular uptake.

Keywords

liposome; cancer; targeting; lipid; cell signaling; metabolism

Introduction

Breast cancer is the most prevalent cancer among women [1]. Triple-negative breast cancer (TNBC) is a subset of this disease, in which the malignant cells do not display estrogen, progesterone, or HER2 receptors on their membrane. These receptors are leveraged for targeting medicines to breast cancer; in their absence, medicinal options become limited and the prognosis of TNBC patients, poor [2].

Nanotechnology is widely used in breast cancer management [3–10], offering improved diagnostic accuracy and therapeutic efficacy [11–13]. Liposomes are vesicles composed of a lipid bilayer that surrounds an inner aqueous core [14]. Hydrophilic drugs can be loaded into the liposomal aqueous core, hydrophobic drugs can be incorporated into the lipid bilayer, and proteins can transcend both regions [15]. Nanoscale liposomes are applied as drug carriers in first-line breast cancer management [16–20]. Tailoring liposome towards improved uptake by TNBC cells may offer new treatment modalities for this condition.

Liposomes can be composed of various lipids, as long as they obey structural laws for configuring a stable bilayer [21, 22]. A dimensionless Packing Parameter (PP) describes the architectural nature of each lipid: $PP=V/(A*L)$; where V is the volume of the hydrophobic lipid tail, 'A' is the cross sectional area of the hydrophilic head, and L is the length of the lipid tails [21]. To construct stable liposomes the average PP of the lipids constituting the bilayer must be between 0.7 to 1.2 [14], and the length of the acyl chains should be between 14 and 22 carbons. Phosphatidylcholine (PC) is a common liposomal building block, participating in a structural, metabolic and cell-signaling processes. PC can be supplemented with other types of lipids to modify the membrane properties [23]. For example, to rigidify the bilayer and reduce its permeability, the bilayer can be enriched with sterols, such as cholesterol [22, 24].

The lipid bilayer can be in several physical states, depending primarily on its composition and on the temperature of the system. Below the phase transition temperature (T_m) the lipid bilayer is in a solid-ordered phase (SO, also known as the ordered gel phase and L_β). Above the T_m the lipid bilayer transforms to the liquid-disordered phase (LD, also known L_α). Adding cholesterol to the lipid bilayer (usually above ~30mol%) the bilayer assumes a liquid-ordered phase (LO) [14].

To improve targeting to disease sites the corona of the liposomes has been decorated with targeting moieties that bind specifically to cancer cells [25–27]. Alternatively, to 'disguise' the liposomes from the immune system and to increase circulation time, polyethylene glycol (PEG) and other polymers have been conjugated to the liposome surface [7, 28]. Several

recent comprehensive studies have addressed the effect PEG has on cellular uptake [29–31], however the effect lipids have on the cellular uptake has not been studied thoroughly [16], especially for the case of triple-negative breast cancer [32].

Here, we investigated how various lipid components affect the uptake of 100-nm liposomes, i.e. lipid nanoparticles by triple-negative breast cancer cells. For that, we screened lipids in a systematic manner, altering different segments of the molecule, and testing each segment's effect on cellular uptake, as well as the cellular viability after engulfing these nanoparticles.

Materials and Methods

Materials

DMPC(1,2-dimyristoyl-sn-glycero-3-phosphocholine,) DPPC(1,2-dipalmitoyl-sn-glycero-3-phosphocholine), HSPC(hydrogenated soybean phosphatidylcholine),DOPC(1,2-dioleoyl-sn-glycero-3-phosphocholine,) DOPS(1,2-dioleoyl-sn-glycero-3-phospho-L-serine),DOPA(1,2-dioleoyl-sn-glycero-3phosphate),DSPE(1,2-Distearoyl-sn-glycero-3-phosphoethanolamine,) DSPG(1,2-distearoyl-sn-glycero-3-phospho-(1'-rac-glycerol), PEG2000-DSPE ((1,2-distearoyl-sn-glycero-3-phosphoethanolamine-N[amino(polyethylene glycol)-2000])were all purchased from Lipoid (Ludwigshafen, Germany). Cholesterol, Hoechst, and pyranine (1-hydroxypyrene-3,6,8-trisulfonic acid) were purchased from Sigma-Aldrich (Revohot, Israel). Rhodamine-DSPE and DLPC (1,2-dilauroyl-sn-glycero-3-phosphocholine) were obtained from Avanti Polar Lipids (Al, USA).

Cell culture

4T1 cells, a mammary carcinoma cell line was purchased from ATCC [33]. The cells were grown in either DMEM/RPMI medium, supplemented with 10% FCS and 1% of L-glutamine, penicillin and streptomycin.

Liposome preparation

Liposomes were prepared by ethanol injection method and subsequent extrusion [34]. In brief, lipids were dissolved in absolute ethanol at 65°C, mixed with 35mM pyranine in buffer (10mM HEPES, 100mM NaCl, pH 7.4), then extruded through polycarbonate membranes (Whatman, Newton, MA, USA) with pore sizes of 400, 200 and 100 nm. Particle size was determined using dynamic light scattering (ZSP Particle Sizer, Malvern, UK). Unencapsulated substance was removed by 12–14 kDa dialysis membrane (Spectrum Labs, Breda, Netherlands) against isosmotic buffer (10mM HEPES, 150mM NaCl, pH 7.4). Rhodamine labeled liposomes were also prepared at the same method. 16:0 Liss Rhod PE or 14:0 Liss Rhod were added to the lipid mixture at 0.1% molar ratio. When lipids used were not soluble in ethanol (different head group experiment), the phospholipids were first dissolved in chloroform and then evaporated using a rotary evaporator (Rotavap R-210, Buchi, Flawil, Switzerland). The created film was rehydrated in the encapsulate solution and then extruded through polycarbonate membranes as described above. HSPC, DMPC, DPPC, and DLPC (100% mol, 100mM) liposomes for flow cytometry analysis and viability test were prepared after lipid dissolution in ethanol at 70°C,40°C,60°C and 40°C respectively.

The molar ratio, size, PDI and zeta-potential measurements of the prepared liposomes are presented in Table S2 (supplementary, Formulations 1-16).

Lipid concentration

High pressure liquid chromatography (HPLC) was implemented to measure the lipid composition and concentration of each liposomal formulation. *Instrumentation and Chromatographic apparatus:* The device used was HPLC (1260 infinity, Agilent Technologies, Santa Clara, California, USA) equipped with a quaternary pump system, auto sampler, a column heater, a diode array UV detector and an ELSD. *Chromatographic conditions:* Lipid separation was completed using Agilent Poroshell 120 EC-C18 4.6x50 mm 2.7-micron column preheated to 45° employing the method of Shibata et al (2013). The mobile phase consisted of two solutions; A 4mM ammonium acetate buffer (pH 4.0) and B 4mM ammonium acetate in methanol, at flow rate of 1ml/min. The starting conditions were a mixture of 20% A and 80% B followed by a linear gradient up to 100% B for 10 min. Then following 10 min at 100% B, the solvent composition gradually returned to the opening conditions after 5 min. ELS detector settings were defined at appropriate temperature and nitrogen flow to evaporate the samples at a temperature of 40°C, gas flow rate of 1.60SLM and of gain 1.0 in order to evaporate the samples properly. Sample injection volume was 20µl Liposome samples were injected after dilution of either 1:100 or 1:50 in dialysis buffer, along with suitable standards mixtures (Figure S1).

Application of liposomes to 4T1 cells

4T1 cells were seeded on 96 well-plate at density of 2×10^4 cells per well at volume of 200µl and incubated at 37°C and 5% CO₂ overnight. Liposomes of different compositions were incubated with the cells. At each time point, the media was removed and cells were washed with PBS. Liposome formulations were diluted according to lipids' concentrations determined by HPLC (with Lipid concentration calibrated from HPLC output presented in Figure S1(B), supplementary. PBS buffer to a final concentration of 100µM lipids and placed on cells for various incubation times. In some experiments (confocal, flow cytometry and MTT), cells were incubated with liposomes after dilution with the media (~10%) to reach final lipid concentration of 5mM.

Uptake determination by fluorescence spectroscopy

At predetermined time points, the cells were washed three times with cold PBS to rid of unassociated liposomes followed by addition of 10mM EDTA. After 10 min incubation at 37°C, cells were detached and transferred to 96 flat bottom black polystyrene plate for fluorescence reading according to pyranine spectra (excitation=415nm (pH-independent), emission 510nm), the fluorescence measured correlated to the total amount of liposomes affiliated with the cells whether bound or internalized (Figure S2, supplementary). The uptake for each formulation was determined by pyranine fluorescence intensity after 100µM liposome application to cells. To obtain the uptake ratio, the values were normalized to the Fluorescence value (uptake) obtained by the reference formulation (Table S2, formulation 1, supplementary).

Evaluation of liposomes' cellular uptake using Flow cytometry

4T1 cells were seeded onto 24-well plate at density of 8×10^4 cells per well in 0.5ml RPMI and allowed to attach overnight (37°C , 5% CO_2). Fluorescent liposomes (labeled with Rhodamine Excitation 570nm, emission 590nm) were applied for 1, 4, 16 and 24 hours. Then, cells were washed with PBS, detached using trypsin and centrifuged with PBS at 500xg for 5 min. The samples measured with BD FACSAria-IIIu cell sorter (laser 561nm and 610/20 (Red) filter), the results were analyzed using FCS Express software.

Liposomes and 4T1 cancer cells viability

4T1 cells were seeded onto 96-well plate at 2.5×10^4 cells in 200 μl medium per well and allowed to attach overnight, liposomes were diluted in cell culture media to achieve final concentration of 5mM and applied to cells for 48-hour incubation at 37°C , 5% CO_2 . Then, MTT assay (Sigma-Aldrich (Revohot, Israel)) was used to measure cell viability. Cell viability of liposomes' treated cells was normalized to the viability of untreated cells.

Growth rate of 4T1 cells

To follow up cancer cells' growth rate after incubation with different lipid based liposomes, InCell 2000 analyzer was used. 4T1 cells were seeded onto 96-well plate at density of 1.25×10^4 cells per well (200 μl). 5 min before reading, nucleus staining using Hoechst (1 $\mu\text{g}/\text{ml}$) was conducted. Cells were counted at three-time points, T_0 (before liposomes addition), 24 and 48 hours after incubation with liposomes. Using INCell investigator software, cells were counted according to Hoechst staining and normalized to their number at T_0 to obtain the growth rate.

Membrane integrity assay using propidium iodide

Propidium iodide (PI) stains dead cells as a result of porous membrane. Once entered the cells, PI binds to DNA increasing its fluorescence. Cells were incubated with DMPC liposomes for 20,28,42 and 52 hours. Then PI reagent was diluted to 2.5 μM with warm PBS and added to the cells. After incubation of 30 min at (37°C , 5% CO_2), PI fluorescence intensity was measured by spectrophotometer (Infinite M200PRO Tecan multimode microplate reader) (Excitation 535nm and Emission 617nm). The values obtained were normalized to DMPC liposomes 100% mol values.

Cell cycle assay by flow cytometry

4T1 cells were seeded onto 24-well plate at density of 8×10^4 cells per well in 0.5ml RPMI and allowed to attach overnight. HSPC, DPPC and DMPC (100% mol) liposomes were applied to the cells for 20-hour incubation. Cells were washed, detached and centrifuged as described before. Cells were resuspended in 100 μl cold PBS, then 1ml 70% ethanol were slowly added and followed by vortex. Cells were incubated on ice for 20 min and centrifuged at 400xg for 5 min. cells were resuspended in PI master mix (1ml= (40 μl PI(1mg/ml), RNase 10 μl (10mg/ml) and 950 μl PBS) at final concentration of 0.5×10^6 cells/ml. After 30 min incubation at RT, cells were analyzed using BD LSR-II Analyzer (Biosciences, San Jose, CA, USA). Results were analyzed using Cell cycle analysis program in FCS Express (De Novo software).

Liposome visualization using Confocal microscopy

Cells were seeded on 8 wells μ -slide (Ibidi) at density of 4×10^4 cells per well in 700 μ l medium. Labeled liposomes were prepared, by incorporating Rhodamine labeled lipid (16:0 Liss Rhod PE or 14:0 16:0 Liss Rhod) into liposome. liposome was diluted in cell medium (10%) and added to cells for 48 hours. After incubation, cells were washed three times with PBS. Then, cell membrane was stained using biotin streptavidin-Alexa Fluor 488 staining, cell nucleus was stained using Hoechst (1 μ g/ml). Cells were viewed using LSM 710 laser scanning Confocal microscope (Zeiss, Oberkochen, Germany). Acquisition was performed using the ZEN software and applying the 405nm, 488nm and 543nm lasers.

Cell lipid extraction

Lipids were extracted according to the method of either Folch or Bligh and dyer [35]. Briefly, for 1ml cell sediment, 3.75ml of 1:2 chloroform: methanol was added and 1.25 ml of chloroform and DDW, each step was followed by vortex. The sample was then centrifuged at 200xg for 5min. A two phase system was created and the bottom organic phase containing the lipids was collected. The solvent was evaporated using rotavapor R-100 (Buchi, Switzerland) and extracted lipids were dissolved in chloroform.

Cancer cells' Lipid composition and detection

Lipid samples were dissolved in chloroform and 10 μ l samples were placed on Thin layer chromatography (TLC) silica gel 60 F254 glass plate (Merck Millipore, Germany), along with known standards (Avanti, Alabaster, Alabama). The spots were dried and the plates were developed at room temperature in mobile phase composed of CHCl_3 : EtOH: H_2O : Et_3N (30:35:7:35) or CHCl_3 : MeOH: H_2O (65:25:4). For *Lipid detection*, the plates were fully dried and stained to detect the lipids on the plate. General stain copper sulfate (10% copper sulfate II in 10% phosphoric acid) was used to observe all lipids in the sample. The phospholipid specific stain molybdenum blue was used to detect phosphate containing lipids, Figure S3.

CryoTEM images of the liposomes

DPPC and DMPC lipid dispersions at concentration of 5 mM were prepared at controlled-environment verification system at 25°C and relative humidity of 100%. Samples were examined using Philips CM120 9 cryo-electron microscope operated at 120 kV. The specimens were equilibrated in below -178°C, then acquired at low-dose imaging mode to minimize electron beam radiation damage, and recorded at a nominal under focus of 4–7 nm to enhance phase contrast an Oxford CT-3500 cooling holder was used. Images were recorded digitally by a Gatan MultiScan 791 CCD camera using the Digital Micrograph 3.1 software package.

Results and Discussion

Triple-negative breast cancer (TNBC) has limited treatment modalities . Nanoliposomes are lipid-based vesicles that are widely used for cancer diagnostics and targeted drug and gene delivery [4, 5, 11, 23, 36–43]. Here, we studied the effect different lipid components have on the uptake of nano-liposomes by TNBC cells. We conducted a systematic screen, testing

how different segments of the lipid molecules, including the headgroup, the acyl tails, and excipients used for stabilizing liposomes, affect nano-liposomal uptake, Figure 1A, Table S2 supplementary.

To test the effect the lipid headgroup has on the cellular uptake we compared 100-nm 100 μ M liposomes composed of hydrogenated soybean phosphatidylcholine (HSPC), to liposomes having a serine headgroup (in phosphatidylserine, PS), or an amine (in phosphatidylethanolamine, PE), or glycerol (in phosphatidylglycerol, PG), or phosphatidic acid (PA) headgroup. Among lipids having the same chain length and level of saturation of 18:0, PE showed greater uptake than PC, which in turn, was slightly superior to PG. The cationic amine head group on PE increased nanoparticle' uptake by 2-fold. Previous studies have shown that the amine headgroup interacts electrostatically with negatively charged lipids and glycans on the cancer cell membrane [44], or, alternatively, the amine headgroup may bind serum proteins that facilitate the trafficking of the particles to unspecific endocytic receptors on the cancer cell [45]. In non-phagocytic cells, negative charge on the particle has been shown to reduce cellular uptake due to electrostatic repulsion between the negatively-charged particle and the negatively-charged cell membrane. This can explain the lower uptake of the anionic PG-nanoparticles compared to zwitterionic PC. When comparing PA and PS, both having similar 18:1 lipid tails, PA demonstrated a significantly 4-fold greater uptake. This can be explained by PA's receptor-driven signaling role in breast cancer [46]. For example, PA has been shown to trigger survival and migration cascades by activating the mTOR, Ras, MEK, ELK and EGFR pathways [47–50]. PA was also shown to promote lipid insertion into cells by enhancing dynamin-based membrane remodeling, which plays a role in receptor-mediated endocytosis [51]. In addition, PA has been shown to affect local membrane curvature, thereby facilitating membrane bending and fusion during endocytosis [52]. These findings can together explain the enhanced uptake of PA liposomes.

These data suggest that targeting cell-specific receptors generates greater uptake compared to unspecific binding to the cell [53]. Triple negative breast cancer (TNBC) cells are characterized by low, or absence, of the expression of hormone receptors for progesterone, estrogen and human epidermal growth factor receptor II (HER2), thereby limiting therapeutic targeting options [54, 55]. However, recent studies show that alternative targeting approaches can be used to improve specificity towards TNBC. Overexpressed cell-surface ligands such as EPCAM (epithelial cell adhesion molecule), epithelial growth factor receptor (EGFR), intercellular adhesion molecule–1(ICAM1) have been used for improving targeting to TNBC tumors in vivo, and even clinically [55, 56]. However, these ligands are not overexpressed in all TNBC tumors or patients. Therefore, effective targeting should be based on a molecular diagnosis of the biomarkers expressed by each patient's tumor, and then, based on the patient's own expression profile targeted medicine should be engineered to treat the patient's own tumor. The acyl chain length of the lipids composing the liposomes also affected the cellular uptake. Specifically, lipids with longer (18:0, HSPC) acyl chains showed greater uptake compared to DPPC (16:0) and DMPC (14:0), respectively, Figure 1D. Furthermore, incorporating an unsaturated lipid (DOPC, 18:1) in the liposome, enhanced the cellular uptake compared to liposomes composed solely of HSPC (18:0), Figure 1C. As the tail lengths of saturated lipids increase, the phase transition temperature (T_m) of the lipid bilayer increases respectively (HSPC,18:0,52°C>DPPC,16:0,41°C>DMPC,14:0,23°C) [57].

Introducing a single unsaturated bond to the lipid tail (18:1) significantly reduces its phase transition temperature to -17°C [58]. These data suggest that the length of the lipid tail, as well as its saturation state, both play an important role in facilitating cellular uptake. Cancer cells have an increased abundance of oleic (18:1) and palmitoleic (16:1) acids, Table S1, supplementary. The enhanced cellular uptake of lipids with long unsaturated tails may be explained by their similarity to the lipids in the cancer cell.

Cholesterol is a common molecular additive in lipid-based drug delivery systems, rigidifying the membrane and enhancing its stability [22, 24]. DMPC liposomes (14:0, $T_m = 24^{\circ}\text{C}$)[57] enriched with cholesterol showed improved cellular uptake, Figure 2B. Contrarily, HSPC liposomes (18:0, $T_m = 52^{\circ}\text{C}$)[59] enriched with cholesterol demonstrated a reduced cellular uptake, Figure 2A. This occurred both at 37 and 4°C ; at 37°C both endocytosis and fusion cellular uptake mechanisms are active, while at 4°C endocytosis is retarded [60, 61]. HSPC has a phase transition temperature of 52°C , granting the liposome a faceted and rigid structure at physiological temperature ($T_m > 37^{\circ}\text{C}$), Figure 2C [62]. Hard and faceted particles have been shown to have improved endocytic uptake compared to round and soft particles [63–65]. Adding cholesterol to HSPC transforms the hard and faceted membrane to a rigid and rounded structure, due to transforming the membrane from a solid-ordered phase to a liquid-ordered phase [66]. This cholesterol-induced structural transformation, from a faceted to a rounded membrane, was imaged using cryoTEM, Figure 2C(I). DMPC's phase transition temperature is 24°C , forming soft and rounded liposomes at physiological temperatures, Figure 2C(II). This structure, in which the lipid bilayers are in a liquid disordered phase, is less favorable for cellular uptake [63–65]. Adding cholesterol to DMPC liposomes rigidifies the membrane transforming it to a liquid-ordered phase, resulting in improved cellular uptake, Figure 2C(II) [63, 67–69]. Uptake experiments at 37°C demonstrate a decline in HSPC internalization when supplemented with cholesterol, suggesting that endocytosis of rigid and rounded particles is less efficient compared to endocytosis of the faceted and solid particles. Contrarily, DMPC uptake increased at 37°C , when supplemented with cholesterol. Soft DMPC particles without cholesterol are taken up mainly by fusion rather than by endocytosis. Evident of this, is the similar uptake level of DMPC liposomes without cholesterol, at both 4 and 37°C . When supplemented with cholesterol, DMPC liposomes demonstrated a significant increase in uptake at 37°C , which is indicative of endocytosis. The uptake of DMPC and HSPC liposomes, with and without cholesterol, by fusion or by endocytosis, was confirmed using confocal microscopy (discussed below in Figure 4). Our results suggest that the effect of cholesterol enrichment is lipid dependent, affecting both cellular uptake and cell viability. Adding cholesterol to DMPC liposomes, gradually cancelled their toxic effect on TNBC cells (Figure 3C). Contrarily, when 40% cholesterol was added to HSPC and DPPC liposomes the cell viability was not as elevated as in cells treated with the cholesterol-free formulation (Figure 3A).

To summarize, cholesterol decreases the membrane fluidity and increases its rigidity [67, 68]. Hard and faceted particles have been shown to be preferable for cellular uptake compared to soft and round particles [63]. To improve cellular uptake, the rigidity and configuration of the nanoparticles should be accounted for [63, 69, 70].

Then we tested the effect of the concentration of the particles in the cell media on the cellular uptake. As the concentration of particles in the cell culture media increases, the total number of particles per cell increased, Figure 2D(I). However, interestingly, as the concentration of particles in the media increased the *uptake efficiency* (i.e., the fraction of particles in solution taken up by cells), decreased, Figure 2D(II). This suggests that as the number of particles taken up by cells increases, the efficiency of the endocytosis process decreases. The reduced efficiency at higher concentrations may be explained by the ability of the cell membrane to conduct a finite number of endocytosis events simultaneously [71, 72]. *In vitro* studies are usually conducted in an environment having a great excess of nanoparticles-per-cell. Efficiency of the drug delivery process must take into account the number of particles that need to enter each cell in order to achieve the therapeutic outcome.

Cancer cell proliferation requires the formation of new membranes; thus, tumor cells activate *de novo* lipid synthesis in order to supply their proliferation needs [73]. Even though lipogenesis is accelerated in cancer cells [74], their rapid proliferation requires also exogenous lipid sources [75]. Therefore, cancer cells source lipids from their microenvironment to supply the metabolic needs and increase proliferation [75–78]. Aggressive cancers have been shown to source more exogenous lipids compared to less aggressive ones [75]. In this study, the correlation between liposomal uptake and their effect on cancer cell proliferation was also addressed. Interestingly, we noticed that liposomal uptake affected the proliferation of cancer cells. Liposomes, taken up by the cancer cells become a source of lipids, fueling cellular proliferation. We noticed that while proliferation increased in cancer cells treated with phospholipids (5mM) having 18 or 16-carbon-long tails (HSPC and DPPC, respectively), cells treated with 14- or 12-carbon-long lipids (DMPC and DLPC) had decreased proliferation, Figure 3. Confocal microscopy demonstrated that the membranes of cells treated with DMPC or DLPC were destabilized, while cells treated with HSPC remained intact, Figure 4. The short acyl chains do not integrate well among the longer lipid chains that are naturally present in the cancer cells. Adding cholesterol to the DMPC formulation cancelled this effect, Figure 3C. Cholesterol is found abundantly in the cell membrane and is a key component in membranes phase behavior. When added to DMPC, cholesterol may stabilize the cell membrane, overcoming the destabilizing effect of DMPC alone, Figure 4A [79, 80]. DMPC destabilizing effect was noticed at 0.5mM and higher concentrations, Figure 3D. The HSPC proliferative effect was also examined at wider concentration range, where a 20-35% increase in cell viability was detected, Figure XX, supplementary. Cell membrane integrity was examined also using the cell-impermeable intercalating fluorescent dye – propidium iodide. DMPC-treated cells showed an increasing fluorescent signal over time, indicative of an increased membrane permeability, compared to the fluorescent signal of DMPC-cholesterol liposomes, Figure 3F. Confocal microscopy, Figure 4, and temperature dependent uptake, Figure 2, tests also suggest that DMPC-cholesterol liposomes are taken up through endocytosis, while DMPC liposomes alone fuse to the cells. Moreover, cells treated with HSPC showed increased proliferation, having 18% \pm 5 of cells in the G2 (premitosis) phase, compared to 8% \pm 2 of untreated cells in G2, Figure 3G. These findings indicate that liposome lipids can be taken up and utilized by the cells to perform metabolic growth related processes.

While cell internalization is a prerequisite for the proper activity of many nanomedicines, it is only the first step. Tuning the particle composition can alter the uptake mechanism, shifting from endocytosis to fusion [81, 82]. Inside the cell, escaping the endosome without compromising the integrity of the drug is critical for facilitating proper therapeutic activity [81, 83, 84]. Targeting intracellular organelles, such as the nucleus or mitochondria, will allow developing new and more sophisticated drugs that treat the proteome and repair metabolic pathways.

Conclusions

Liposomes and other nanotechnologies are emerging medical tools, owned to their ability to target therapeutic and diagnostic agents to diseased tissues [5, 16, 36, 85–89]. This study demonstrates that the uptake of liposomes by triple-negative breast cancer cells can be tuned by selecting the lipid composition and concentration (Table 1). We found that using phosphatidic acid (PA) in the liposome formulation had the greatest uptake effect compared to unspecific cellular binding moieties. Furthermore, the degree of lipid's chain saturation affects cellular uptake, specifically, the monounsaturated phospholipid DOPC(18:1) was superior to saturated lipids of the same length. Among lipids with saturated tails, HSPC (18:0) was superior to shorter saturated lipids. The natural lipid composition of breast cancer cells has high levels of long monounsaturated lipids, possibly explaining why liposomal lipids of a similar molecular composition grant enhanced cellular uptake [90, 91]. Longer lipids such as HSPC(18:0) and DPPC(16:0) promoted proliferation, while the shorter lipids, DMPC(14:0) and DLPC(12:0), destabilized the cell membrane resulting in cell death.

In summary, we show here that the liposomal composition affects the cellular fate and viability, emphasizing the importance of tailoring the lipid composition of nanoparticles in order to achieve the desired therapeutic outcome

Supplementary Material

Refer to Web version on PubMed Central for supplementary material.

Acknowledgments

This work was supported by ERC-STG-2015-680242.

The authors also acknowledge the support of the Technion Integrated Cancer Center (TICC), the Russell Berrie Nanotechnology Institute, the Lorry I. Lokey Interdisciplinary Center for Life Sciences & Engineering especially Dr. Nitsan Dahan and Dr. Yael Lupu-Haber, The Israel Ministry of Economy for a Kamin Grant (52752); the Israel Ministry of Science Technology and Space – Office of the Chief Scientist (3-11878); the Israel Science Foundation (1778/13, 1421/17); the Israel Cancer Association (2015-0116); the German-Israeli Foundation for Scientific Research and Development for a GIF Young grant (I-2328-1139.10/2012); the European Union FP-7 IRG Program for a Career Integration Grant (908049); the Phospholipid Research Center Grant; a Mallat Family Foundation Grant; The Unger Family Fund; A. Schroeder acknowledges Alon and Taub Fellowships. We also thank E. Kesselman and Irena Davidovitch for assisting in acquiring CryoTEM images of the liposomes. H. Abumanhal and N. Krinsky wish to thank the Baroness Ariane de Rothschild Women Doctoral Program for its generous support.

References

- [1]. Siegel RL, Miller KD, Jemal A. Cancer statistics, 2016. *CA Cancer J Clin.* 2016; 66:7–30. [PubMed: 26742998]

- [2]. Isakoff SJ. Triple-negative breast cancer: role of specific chemotherapy agents. *Cancer J*. 2010; 16:53–61. [PubMed: 20164691]
- [3]. Schroeder A, Heller DA, Winslow MW, Dahلمان JE, Pratt GW, Langer R, Jacks T, Anderson DG. Treating metastatic cancer with nanotechnology. *Nature Rev Cancer*. 2011; 12:39–50. [PubMed: 22193407]
- [4]. Peer D, Karp JM, Hong S, Farokhzad OC, Margalit R, Langer R. Nanocarriers as an emerging platform for cancer therapy. *Nat Nanotechnol*. 2007; 2:751–760. [PubMed: 18654426]
- [5]. Duncan R, Gaspar R. Nanomedicine(s) under the microscope. *Mol Pharm*. 2011; 8:2101–2141. [PubMed: 21974749]
- [6]. Fleige E, Quadir MA, Haag R. Stimuli-responsive polymeric nanocarriers for the controlled transport of active compounds: concepts and applications. *Adv Drug Deliv Rev*. 2012; 64:866–884. [PubMed: 22349241]
- [7]. Luxenhofer R, Schulz A, Roques C, Li S, Bronich TK, Batrakova EV, Jordan R, Kabanov AV. Doubly amphiphilic poly(2-oxazoline)s as high-capacity delivery systems for hydrophobic drugs. *Biomaterials*. 2010; 31:4972–4979. [PubMed: 20346493]
- [8]. Torchilin VP. Multifunctional, stimuli-sensitive nanoparticulate systems for drug delivery. *Nature Reviews Drug Discovery*. 2014; 13:813. [PubMed: 25287120]
- [9]. Tsvetkova Y, Beztsinna N, Baues M, Klein D, Rix A, Golombek SK, Al Rawashdeh We, Gremse F, Barz M, Koynov K, Banala S, et al. Balancing Passive and Active Targeting to Different Tumor Compartments Using Riboflavin-Functionalized Polymeric Nanocarriers. *Nano letters*. 2017; 17:4665–4674. [PubMed: 28715227]
- [10]. Talelli M, Rijcken CJF, Oliveira S, van der Meel R, van Bergen en Henegouwen PMP, Lammers T, van Nostrum CF, Storm G, Hennink WE. Nanobody — Shell functionalized thermosensitive core-crosslinked polymeric micelles for active drug targeting. *Journal of Controlled Release*. 2011; 151:183–192. [PubMed: 21262289]
- [11]. Yaari Z, da Silva D, Zinger A, Goldman E, Kajal A, Tshuva R, Barak E, Dahan N, Hershkovitz D, Goldfeder M, Roitman JS, et al. Theranostic barcoded nanoparticles for personalized cancer medicine. *Nat Commun*. 2016; 7
- [12]. Miller K, Erez R, Segal E, Shabat D, Satchi-Fainaro R. Targeting bone metastases with a bispecific anticancer and antiangiogenic polymer-alendronate-taxane conjugate. *Angew Chem Int Ed Engl*. 2009; 48:2949–2954. [PubMed: 19294707]
- [13]. Lammers T, Kiessling F, Ashford M, Hennink W, Crommelin D, Storm G. Cancer nanomedicine: Is targeting our target? *Nat Rev Mater*. 2016; 1
- [14]. Israelachvili, JN. *Intermolecular and Surface Forces*. 2 ed. Academic Press; London: 1992.
- [15]. Torchilin, V, Weissig, V. *Liposomes: A Practical Approach*. Oxford University Press; 2003.
- [16]. Barenholz Y. Doxil(R)—the first FDA-approved nano-drug: lessons learned. *J Control Release*. 2012; 160:117–134. [PubMed: 22484195]
- [17]. Rizzo LY, Theek B, Storm G, Kiessling F, Lammers T. Recent progress in nanomedicine: therapeutic, diagnostic and theranostic applications. *Curr Opin Biotechnol*. 2013; 24:1159–1166. [PubMed: 23578464]
- [18]. Carmeliet P, Jain RK. Angiogenesis in cancer and other diseases. *Nature*. 2000; 407:249–257. [PubMed: 11001068]
- [19]. Matsumura Y, Maeda H. A new concept for macromolecular therapeutics in cancer chemotherapy: mechanism of tumoritropic accumulation of proteins and the antitumor agent smancs. *Cancer Res*. 1986; 46:6387–6392. [PubMed: 2946403]
- [20]. Harrington KJ, Mohammadtaghi S, Uster PS, Glass D, Peters AM, Vile RG, Stewart JS. Effective targeting of solid tumors in patients with locally advanced cancers by radiolabeled pegylated liposomes. *Clin Cancer Res*. 2001; 7:243–254. [PubMed: 11234875]
- [21]. Kumar VV. Complementary molecular shapes and additivity of the packing parameter of lipids. *PNAS*. 1991; 88:444–448. [PubMed: 1988944]
- [22]. Garbuzenko O, Barenholz Y, Prieve A. Effect of grafted PEG on liposome size and on compressibility and packing of lipid bilayer. *Chem Phys Lipids*. 2005; 135:117–129. [PubMed: 15921973]

- [23]. Torchilin VP. Multifunctional, stimuli-sensitive nanoparticulate systems for drug delivery. *Nat Rev Drug Discov.* 2014; 13:813–827. [PubMed: 25287120]
- [24]. Sivan S, Schroeder A, Verberne G, Merkher Y, Diminsky D, Prieve A, Maroudas A, Halperin G, Nitzan D, Etsion I, Barenholz Y. Liposomes act as effective biolubricants for friction reduction in human synovial joints. *Langmuir.* 2010; 26:1107–1116. [PubMed: 20014818]
- [25]. Torchilin VP. Multifunctional, stimuli-sensitive nanoparticulate systems for drug delivery. *Nat Rev Drug Discov.* 2014
- [26]. Schroeder JE, Shweky I, Shmeeda H, Banin U, Gabizon A. Folate-mediated tumor cell uptake of quantum dots entrapped in lipid nanoparticles. *J Control Release.* 2007; 124:28–34. [PubMed: 17928088]
- [27]. Mehrabadi FS, Adelman J, Gupta S, Wedepohl S, Calderon M, Brinkmann U, Haag R. Bispecific Antibodies for Targeted Delivery of Dendritic Polyglycerol (dPG) Prodrug Conjugates. *Curr Cancer Drug Targets.* 2016; 16:639–649. [PubMed: 26853135]
- [28]. Klibanov AL, Maruyama K, Torchilin VP, Huang L. Amphipathic polyethyleneglycols effectively prolong the circulation time of liposomes. *FEBS Lett.* 1990; 268:235–237. [PubMed: 2384160]
- [29]. Vu VP, Gifford GB, Chen F, Benasutti H, Wang G, Groman EV, Scheinman R, Saba L, Moghimi SM, Simberg D. Immunoglobulin deposition on biomolecule corona determines complement opsonization efficiency of preclinical and clinical nanoparticles. *Nat Nanotechnol.* 2019
- [30]. Needham D, McIntosh TJ, Lasic DD. Repulsive interactions and mechanical stability of polymer-grafted lipid membranes. *Biochimica et biophysica acta.* 1992; 1108:40–48. [PubMed: 1643080]
- [31]. Klibanov AL, Maruyama K, Torchilin VP, Huang L. Amphipathic polyethyleneglycols effectively prolong the circulation time of liposomes. *FEBS Lett.* 1990; 268:235–237. [PubMed: 2384160]
- [32]. Mayer LD, Tai LC, Ko DS, Masin D, Ginsberg RS, Cullis PR, Bally MB. Influence of vesicle size, lipid composition, and drug-to-lipid ratio on the biological activity of liposomal doxorubicin in mice. *Cancer research.* 1989; 49:5922–5930. [PubMed: 2790807]
- [33]. Wagenblast E, Soto M, Gutierrez-Angel S, Hartl CA, Gable AL, Maceli AR, Erard N, Williams AM, Kim SY, Dickopf S, Harrell JC, et al. A model of breast cancer heterogeneity reveals vascular mimicry as a driver of metastasis. *Nature.* 2015; 520:358–362. [PubMed: 25855289]
- [34]. Schroeder A, Avnir Y, Weisman S, Najajreh Y, Gabizon A, Talmon Y, Kost J, Barenholz Y. Controlling liposomal drug release with low frequency ultrasound: mechanism and feasibility. *Langmuir.* 2007; 23:4019–4025.
- [35]. Blich EG, Dyer WJ. A rapid method of total lipid extraction and purification. *Canadian journal of biochemistry and physiology.* 1959; 37:911–917. [PubMed: 13671378]
- [36]. Etheridge ML, Campbell SA, Erdman AG, Haynes CL, Wolf SM, McCullough J. The big picture on nanomedicine: the state of investigational and approved nanomedicine products. *Nanomedicine.* 2013; 9:1–14. [PubMed: 22684017]
- [37]. Stark WJ. Nanoparticles in biological systems. *Angewandte Chemie.* 2011; 50:1242–1258. [PubMed: 21290491]
- [38]. Goldman E, Zinger A, da Silva D, Yaari Z, Kajaal A, Vardi-Oknin D, Goldfeder M, Schroeder JE, Shainsky-Roitman J, Hershkovitz D, Schroeder A. Nanoparticles target early-stage breast cancer metastasis in vivo. *Nanotechnology.* 2017; 28:43LT01.
- [39]. Zinger A, Adir O, Alper M, Simon A, Poley M, Tzror C, Yaari Z, Krayem M, Kasten S, Nawy G, Herman A, et al. Proteolytic Nanoparticles Replace a Surgical Blade by Controllably Remodeling the Oral Connective Tissue. *ACS Nano.* 2018
- [40]. Folkman J. Can mosaic tumor vessels facilitate molecular diagnosis of cancer? *Proc Natl Acad Sci U S A.* 2001; 98:398–400. [PubMed: 11209044]
- [41]. Ojha T, Rizzo L, Storm G, Kiessling F, Lammers T. Image-guided drug delivery: preclinical applications and clinical translation. *Expert opinion on drug delivery.* 2015; 12:1203–1207. [PubMed: 26083469]
- [42]. Theek B, Gremse F, Kunjachan S, Fokong S, Pola R, Pechar M, Deckers R, Storm G, Ehling J, Kiessling F, Lammers T. Characterizing EPR-mediated passive drug targeting using contrast-enhanced functional ultrasound imaging. *Journal of controlled release : official journal of the Controlled Release Society.* 2014; 182:83–89. [PubMed: 24631862]

- [43]. Harrington KJ, Lewanski CR, Northcote AD, Whittaker J, Wellbank H, Vile RG, Peters AM, Stewart JS. Phase I-II study of pegylated liposomal cisplatin (SPI-077) in patients with inoperable head and neck cancer. *Ann Oncol*. 2001; 12:493. [PubMed: 11398881]
- [44]. Kedmi R, Ben-Arie N, Peer D. The systemic toxicity of positively charged lipid nanoparticles and the role of Toll-like receptor 4 in immune activation. *Biomaterials*. 2010; 26:6867–6875.
- [45]. Akinc A, Querbes W, De SM, Qin J, Frank-Kamenetsky M, Jayaprakash KN, Jayaraman M, Rajeev KG, Cantley WL, Dorkin JR, Butler JS, et al. Targeted delivery of RNAi therapeutics with endogenous and exogenous ligand-based mechanisms. *Molecular Therapy*. 2010; 18:1357–1364. [PubMed: 20461061]
- [46]. Lu M, Tay LWR, He J, Du G. Monitoring Phosphatidic Acid Signaling in Breast Cancer Cells Using Genetically Encoded Biosensors. *Methods in molecular biology (Clifton, N.J.)*. 2016; 1406:225–237.
- [47]. Foster DA. Phosphatidic acid signaling to mTOR: signals for the survival of human cancer cells. *Biochim Biophys Acta*. 2009; 1791:949–955. [PubMed: 19264150]
- [48]. Andresen BT, Rizzo MA, Shome K, Romero G. The role of phosphatidic acid in the regulation of the Ras/MEK/Erk signaling cascade. *FEBS Lett*. 2002; 531:65–68. [PubMed: 12401205]
- [49]. Zhao C, Du G, Skowronek K, Frohman MA, Bar-Sagi D. Phospholipase D2-generated phosphatidic acid couples EGFR stimulation to Ras activation by Sos. *Nat Cell Biol*. 2007; 9:706–712. [PubMed: 17486115]
- [50]. Sliva D, Mason R, Xiao H, English D. Enhancement of the Migration of Metastatic Human Breast Cancer Cells by Phosphatidic Acid. *Biochemical and biophysical research communications*. 2000; 268:471–479. [PubMed: 10679229]
- [51]. Burger KNJ, Demel RA, Schmid SL, de Kruijff B. Dynamin Is Membrane-Active: Lipid Insertion Is Induced by Phosphoinositides and Phosphatidic Acid. *Biochemistry*. 2000; 39:12485–12493. [PubMed: 11015230]
- [52]. Kooijman EE, Chupin V, Fuller NL, Kozlov MM, de Kruijff B, Burger KNJ, Rand PR. Spontaneous Curvature of Phosphatidic Acid and Lysophosphatidic Acid. *Biochemistry*. 2005; 44:2097–2102. [PubMed: 15697235]
- [53]. Perche F, Patel NR, Torchilin VP. Accumulation and toxicity of antibody-targeted doxorubicin-loaded PEG-PE micelles in ovarian cancer cell spheroid model. *J Control Release*. 2012; 164:95–102. [PubMed: 22974689]
- [54]. Elkhalfi D, Alali F, Al Moustafa AE, Khalil A. Targeting triple negative breast cancer heterogeneity with chalcones: a molecular insight. *Journal of drug targeting*. 2018:1–9.
- [55]. Jhan J-R, Andrechek ER. Triple-negative breast cancer and the potential for targeted therapy. *Pharmacogenomics*. 2017; 18:1595–1609. [PubMed: 29095114]
- [56]. Jenkins SV, Nima ZA, Vang KB, Kannarpady G, Nedosekin DA, Zharov VP, Griffin RJ, Biris AS, Dings RPM. Triple-negative breast cancer targeting and killing by EpCAM-directed, plasmonically active nanodrug systems. *NPJ precision oncology*. 2017; 1:27. [PubMed: 29872709]
- [57]. Silvius, JR. Thermotropic phase transitions of pure lipids in model membranes and their modifications by membrane proteins. *Lipid-Protein Interactions*. John Wiley & Sons; New York: 1982.
- [58]. Silvius, DJR. Thermotropic Phase Transitions of Pure Lipids in Model Membranes and Their Modifications by Membrane Proteins. *Lipid-Protein Interactions*. John Wiley & Sons; New York: 1982.
- [59]. Lichtenberg D, Barenholz Y. Liposomes: preparation, characterization, and preservation. *Methods Biochem Anal*. 1988; 33:337–462. [PubMed: 3282152]
- [60]. Kabanov AV, Sahay G, Alakhova DY. Endocytosis of nanomedicines. *Journal of Controlled Release*. 2010; 145:182–195. [PubMed: 20226220]
- [61]. Rajaganapathy BR, Chancellor MB, Nirmal J, Dang L, Tyagi P. Bladder uptake of liposomes after intravesical administration occurs by endocytosis. *PLoS one*. 2015; 10:e0122766–e0122766. [PubMed: 25811468]

- [62]. Kim D, Costello M, Duncan P, Needham D. Mechanical properties and microstructure of polycrystalline phospholipid monolayer shells: Novel solid microparticles. *Langmuir*. 2003; 19:8455–8466.
- [63]. Anselmo A, Zhang M, Kumar S, Vogus DR, Menegatti S, Helgeson M, Mitragotri S. Elasticity of Nanoparticles Influences Their Blood Circulation, Phagocytosis, Endocytosis, and Targeting. 2015
- [64]. Banerjee A, Qi J, Gogoi R, Wong J, Mitragotri S. Role of nanoparticle size, shape and surface chemistry in oral drug delivery. *J Control Release*. 2016; 238:176–185. [PubMed: 27480450]
- [65]. Gratton SE, Ropp PA, Pohlhaus PD, Luft JC, Madden VJ, Napier ME, DeSimone JM. The effect of particle design on cellular internalization pathways. *Proc Natl Acad Sci U S A*. 2008; 105:11613–11618. [PubMed: 18697944]
- [66]. Estep TN, Freire E, Anthony F, Barenholz Y, Biltonen RL, Thompson TE. Thermal behavior of stearyl sphingomyelin-cholesterol dispersions. *Biochemistry*.
- [67]. Raffy S, Teissié J. Control of Lipid Membrane Stability by Cholesterol Content. *Biophysical journal*. 1999; 76:2072–2080. [PubMed: 10096902]
- [68]. Barenholz, Y. Sphingomyelin and cholesterol: from membrane biophysics and rafts to potential medical applications *Membrane Dynamics and Domains*. Springer; 2004. 167–215.
- [69]. Guo P, Liu D, Subramanyam K, Wang B, Yang J, Huang J, Auguste DT, Moses MA. Nanoparticle elasticity directs tumor uptake. *Nature communications*. 2018; 9
- [70]. Foroozandeh P, Aziz AA. Insight into Cellular Uptake and Intracellular Trafficking of Nanoparticles. *Nanoscale research letters*. 2018; 13:339–339. [PubMed: 30361809]
- [71]. Zhang S, Li J, Lykotrafitis G, Bao G, Suresh S. Size-Dependent Endocytosis of Nanoparticles. *Adv Mater*. 2009; 21:419–424. [PubMed: 19606281]
- [72]. Akinc A, Battaglia G. Exploiting endocytosis for nanomedicines. *Cold Spring Harb Perspect Biol*. 2013; 5:a016980. [PubMed: 24186069]
- [73]. Zaidi N, Lupien L, Kummerle NB, Kinlaw WB, Swinnen JV, Smans K. Lipogenesis and lipolysis: the pathways exploited by the cancer cells to acquire fatty acids. *Progress in lipid research*. 2013; 52:585–589. [PubMed: 24001676]
- [74]. Kuhajda FP, Pizer ES, Li JN, Mani NS, Frehywot GL, Townsend CA. Synthesis and antitumor activity of an inhibitor of fatty acid synthase. *Proceedings of the National Academy of Sciences of the United States of America*. 2000; 97:3450–3454. [PubMed: 10716717]
- [75]. Louie SM, Roberts LS, Mulvihill MM, Luo K, Nomura DK. Cancer cells incorporate and remodel exogenous palmitate into structural and oncogenic signaling lipids. *Biochimica et Biophysica Acta (BBA) - Molecular and Cell Biology of Lipids*. 2013; 1831:1566–1572. [PubMed: 23872477]
- [76]. Warburg O, Posener K, Negelein E. Ueber den Stoffwechsel der Tumoren. *Biochemische Zeitschrift*. 1924; 152:319–344.
- [77]. Rysman E, Brusselmans K, Scheys K, Timmermans L, Derua R, Munck S, Van Veldhoven PP, Waltregny D, Daniels VW, Machiels J, Vanderhoydonc F, et al. De novo lipogenesis protects cancer cells from free radicals and chemotherapeutics by promoting membrane lipid saturation. *Cancer Res*. 2010; 70:8117–8126. [PubMed: 20876798]
- [78]. Yao CH, Fowle-Grider R, Mahieu NG, Liu GY, Chen YJ, Wang R, Singh M, Potter GS, Gross RW, Schaefer J, Johnson SL, et al. Exogenous Fatty Acids Are the Preferred Source of Membrane Lipids in Proliferating Fibroblasts. *Cell chemical biology*. 2016; 23:483–493. [PubMed: 27049668]
- [79]. Presti FT. The role of cholesterol in regulating membrane fluidity. *Membrane fluidity in biology*. 1985; 4:97–145.
- [80]. Allen TM, Chonn A. Large unilamellar liposomes with low uptake into the reticuloendothelial system. *FEBS letters*. 1987; 223:42–46. [PubMed: 3666140]
- [81]. Stewart MP, Lorenz A, Dahlman J, Sahay G. Challenges in carrier-mediated intracellular delivery: moving beyond endosomal barriers. *Wiley Interdisciplinary Reviews: Nanomedicine and Nanobiotechnology*. 2016; 8:465–478. [PubMed: 26542891]

- [82]. Sahay G, Alakhova DY, Kabanov AV. Endocytosis of nanomedicines. *Journal of controlled release : official journal of the Controlled Release Society*. 2010; 145:182–195. [PubMed: 20226220]
- [83]. Akinc A, Goldberg M, Qin J, Dorkin JR, Gamba-Vitalo C, Maier M, Jayaprakash KN, Jayaraman M, Rajeev KG, Manoharan M, Kotliansky V, et al. Development of lipidoid-siRNA formulations for systemic delivery to the liver. *Molecular therapy : the journal of the American Society of Gene Therapy*. 2009; 17:872–879. [PubMed: 19259063]
- [84]. Varkouhi AK, Scholte M, Storm M G, Haisma HJ. Endosomal escape pathways for delivery of biologicals. *Journal of Controlled Release*. 2011; 151:220–228. [PubMed: 21078351]
- [85]. Hafner A, Lovric J, Lakos GP, Pepic I. Nanotherapeutics in the EU: an overview on current state and future directions. *Int J Nanomedicine*. 2014; 9:1005–1023. [PubMed: 24600222]
- [86]. Weissig V, Guzman-Villanueva D. Nanopharmaceuticals (part 2): products in the pipeline. *Int J Nanomedicine*. 2015; 10:1245–1257. [PubMed: 25709446]
- [87]. Weissig V, Pettinger TK, Murdock N. Nanopharmaceuticals (part 1): products on the market. *Int J Nanomedicine*. 2014; 9:4357–4373. [PubMed: 25258527]
- [88]. Noorlander CW, Kooi MW, Oomen AG, Park MV, Vandebriel RJ, Geertsma RE. Horizon scan of nanomedicinal products. *Nanomedicine (Lond)*. 2015; 10:1599–1608. [PubMed: 25694061]
- [89]. Evers, P. *Nanotechnology in Medical Applications: The Global Market* Healthcare Market Research Reports. BCC Research; 2015.
- [90]. Fermor BF, Masters JR, Wood CB, Miller J, Apostolov K, Habib NA. Fatty acid composition of normal and malignant cells and cytotoxicity of stearic, oleic and steric acids in vitro. *European journal of cancer*. 1992; 28A:1143–1147. [PubMed: 1320912]
- [91]. Meng X, Riordan NH, Riordan HD, Mikirova N, Jackson J, González MJ, Miranda-Massari JR, Mora E, Trinidad-Castillo W. Cell Membrane Fatty Acid Composition Differs Between Normal and Malignant Cell Lines. *Puerto Rico health sciences journal*. 2010; 23

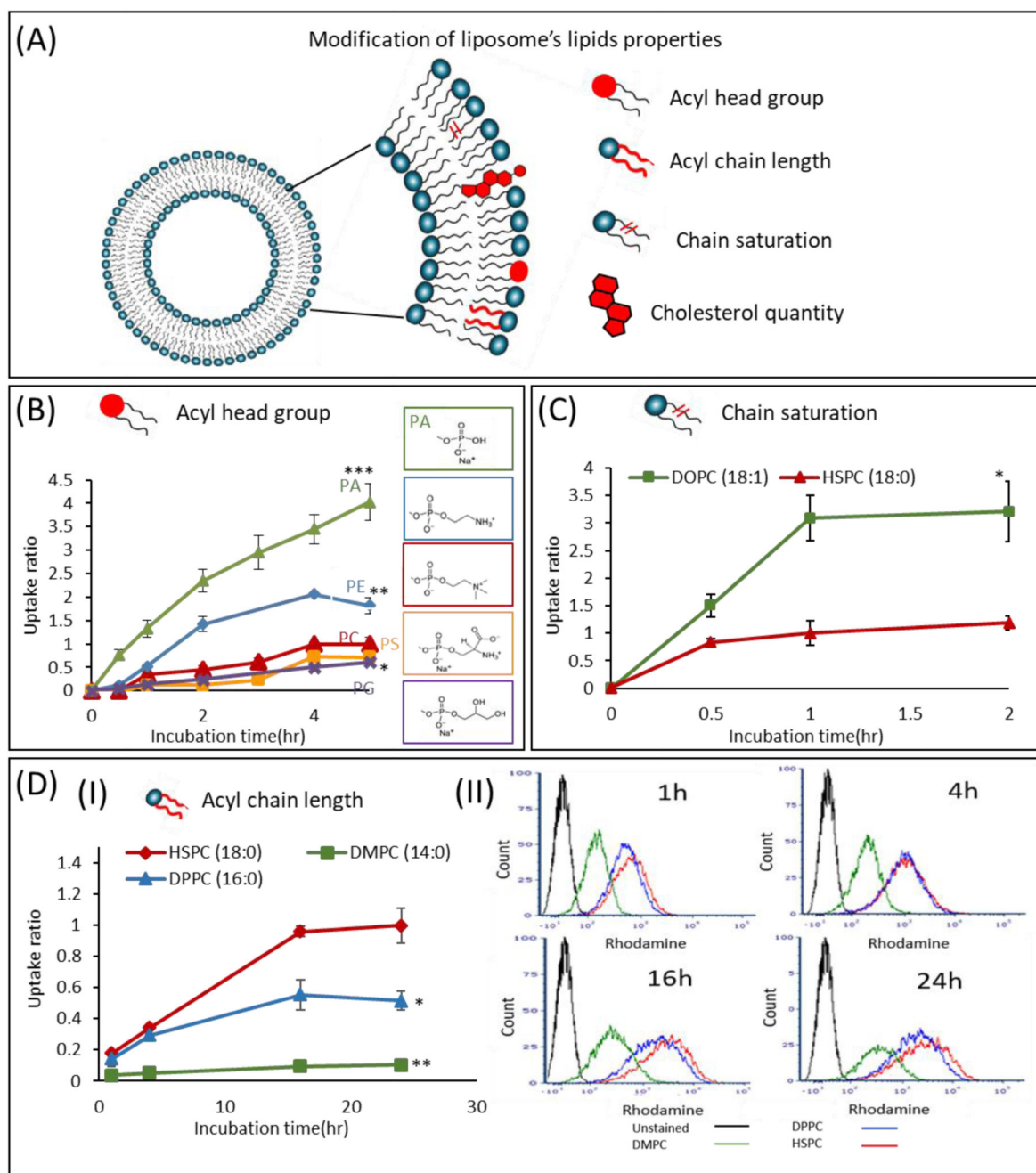


Figure 1. The uptake of liposomes (100 μ M) composed of various lipid compositions by triple negative 4T1 breast cancer cells.

(A) Schematic representation of the systematic screening approach of the study. The effect of lipid head moieties, fatty acid chains length and saturation, and cholesterol on the cellular uptake were studied. (B) The effect of different lipid head groups (PA, PE, PC, PS and PG) on cellular uptake were quantified over time. (C) The effect of the lipid tail fatty acid saturation was compared. (D) The effect of the acyl chain length on cellular uptake was studied. Phospholipids with different fatty acyl chain length (18, 16 and 14-carbon-long tails) were compared (I) over 24 hours, using flow cytometry (II). Error bars represent

standard deviation from 3 independent repeats. *Significant difference between the reference formulation and the other formulations, where * $p < 0.05$, ** $p < 0.01$, *** $p < 0.001$ according to a Student's *t*-test with a two-tailed distribution with equal variance.

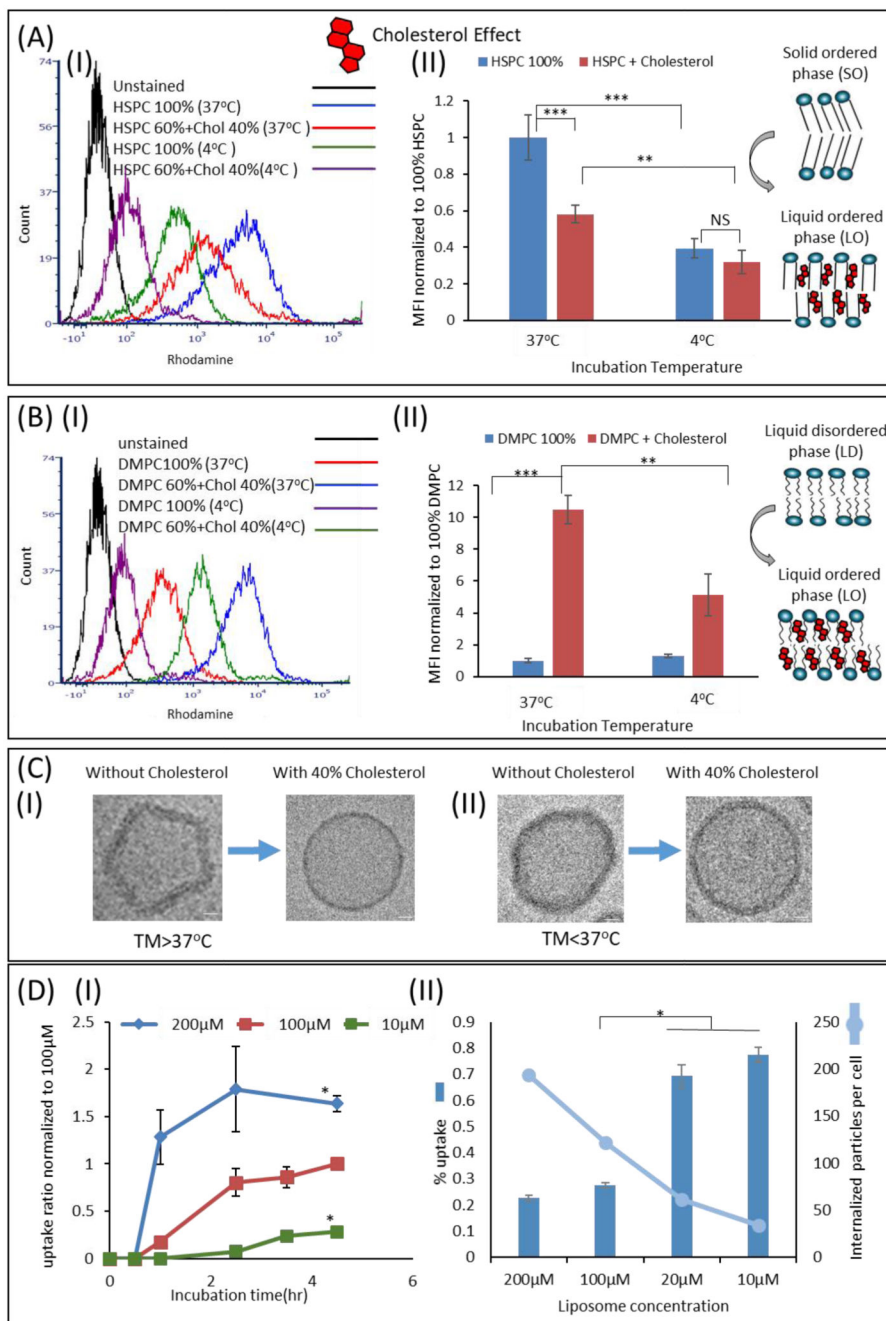


Figure 2. Effect of cholesterol and the ratio of liposomes-per-cell on the cellular uptake. (A, B) The uptake of liposomes composed of HSPC (18:0) or DMPC (14:0), with or without cholesterol, was studied at 4°C and 37°C. (C) CryoTem images of the effect of cholesterol on a DPPC liposome structure, transforming from a faceted to rounded structure upon adding 40mole% cholesterol into the membrane. (II) DMPC liposomes without/with cholesterol (40mole%). Scale bars represent 10nm. (D) (I) 4T1 cells were incubated with HSPC liposomes at increasing concentrations and the uptake was recorded. (II) The *efficiency* of liposomal uptake (the percent of liposomes taken up from the solution relative

to their concentration in the media) was measured. Error bars represent standard deviation from 3 independent repeats. *Significant difference, where $*p < 0.05$, $**p < 0.01$, $***p < 0.001$ according to a Student's t-test with a two-tailed distribution with equal variance.

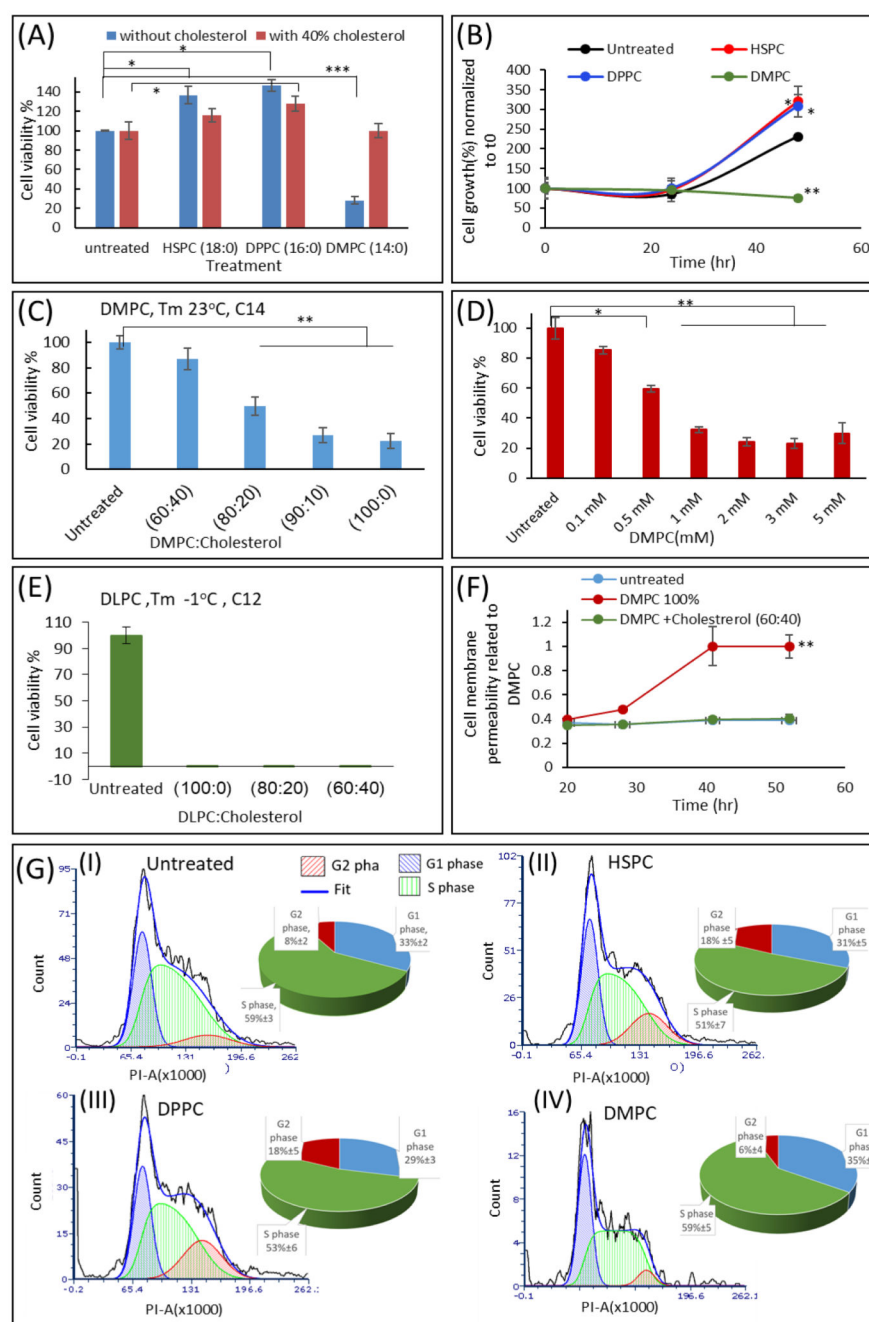


Figure 3. The effect of the liposome lipid composition on the viability of cancer cells. (A) Cancer cell viability 48-hours after incubating with different liposomes(5mM), with and without cholesterol, normalized to the viability of untreated breast cancer cells. (B) Cancer cell proliferation rate as a function of treatment with different formulations. (C) The effect of DMPC liposomes(5mM), enriched with cholesterol at different concentrations, on the viability of triple-negative 4T1 cancer cells. (D) The effect of DMPC liposomes at different concentrations(0.1mM-5mM) on the viability of 4T1 cells. (E) The effect of DLPC (12:0) liposomes on cancer cell viability. (F) Cell membrane permeability, measured using

propidium iodide fluorescence intensity over time after incubating 4T1 cells with DMPC liposomes. (G) Cell cycle analysis by flow cytometry after incubating the cells with HSPC, DPPC and DMPC-liposomes compared to untreated cell. The percentage of cells in the G1 (protein synthesis phase), S (DNA synthesis phase) and G2 (pre mitosis) phases are presented. Error bars represent standard deviation from 3 independent repeats. *Significant difference between the untreated group and the other formulations treated groups, where $*p < 0.05$, $**p < 0.01$, $***p < 0.001$ according to a Student's t-test with a two-tailed distribution with equal variance.

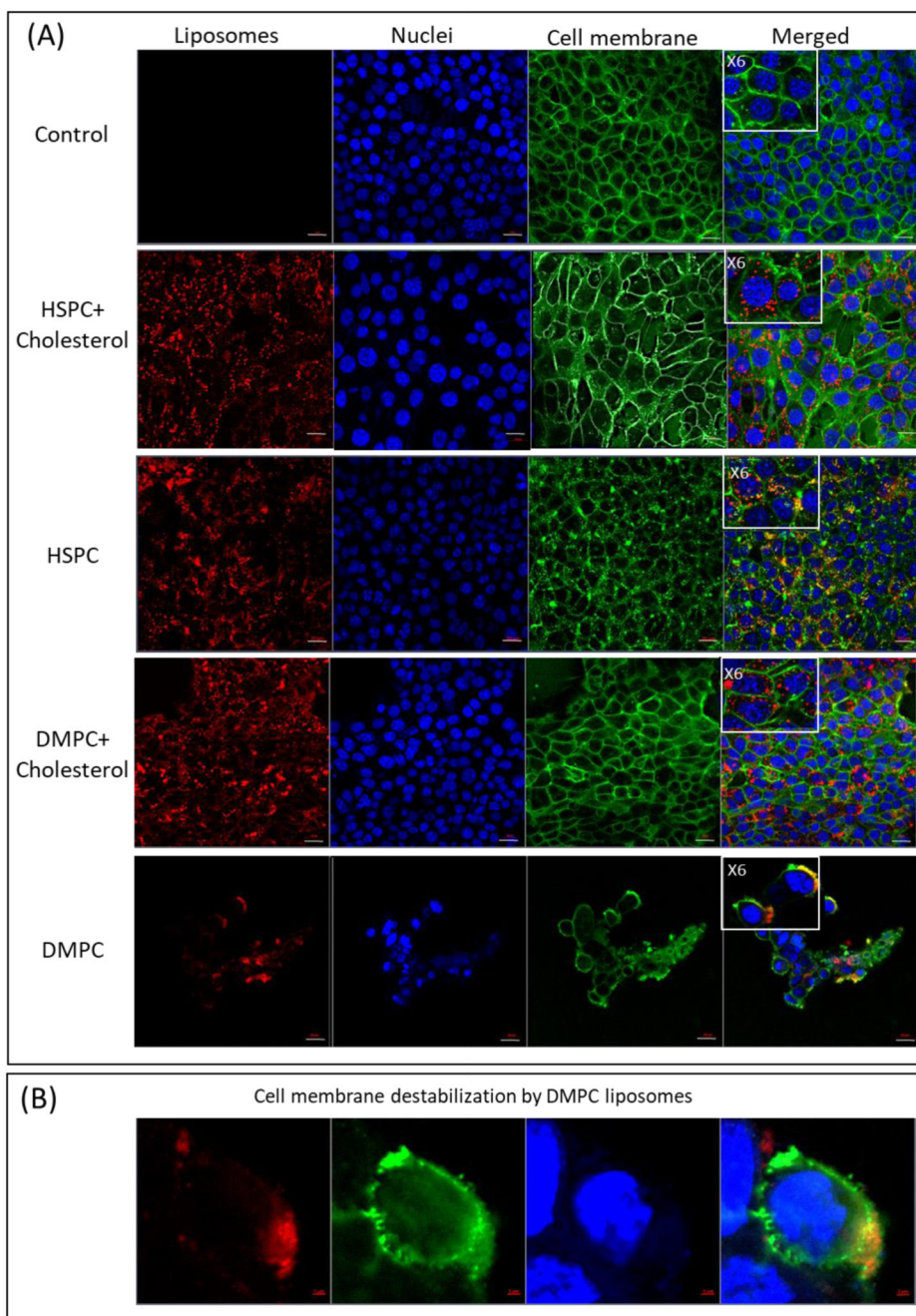


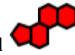



Figure 4. The lipid formulation can destabilize the membrane of the cancer cell.

(A) Representative images of DMPC and HSPC-liposomes (5mM) uptake by 4T1 cells after a 48 hr incubation. Liposome's lipid layer was labeled red (Rhodamine), cell nucleus was labeled blue (Hoechst) and cell membrane was labeled green (Alexa Fluor 488), overlay images, scale bars represent 20 μ m. (B) Representative images demonstrate membrane destabilization after incubation with DMPC-liposomes after 48 hours, scale bars represent 2 μ m.

Table 1
Summarizing the effects different lipid components have on the uptake of liposomes by triple negative breast cancer cells.

Modifying parameter	↑ Increased/ ↓ Decreased uptake
↑ Chain length 	↑
↑ Chain saturation 	↑
↑ Cholesterol 	With DMPC ↑ with HSPC ↓
Head group 	PA, PE ↑ PS, PG ↓